Universality of transport properties of ultra-thin oxide films

V Lacquaniti[1], M Belogolovskii[2], C Cassiago[1], N De Leo[1], M Fretto[1], A Sosso[1]

[1] National Institute of Metrological Research, Electromagnetism Division, Strada delle Cacce 91, 10135 Torino, Italy

[2] Donetsk Institute for Physics and Engineering, National Academy of Sciences of Ukraine, Str. Rosa Luxemburg 72, 83114 Donetsk, Ukraine

E-mail: v.lacquaniti@inrim.it

Abstract. We report low-temperature measurements of current-voltage characteristics for highly conductive Nb/Al-AlO_x-Nb junctions with thicknesses of the Al interlayer ranging from 40 to 150 nm and ultra-thin barriers formed by diffusive oxidation of the Al surface. In a superconducting state these devices have revealed a strong subgap current leakage. Analyzing Cooper-pair and quasiparticle currents across the devices, we conclude that the strong suppression of the subgap resistance comparing with conventional tunnel junctions is not related to technologically derived pinholes in the barrier but rather has more fundamental grounds. We argue that it originates from a universal bimodal distribution of transparencies across the Al-oxide barrier proposed earlier by Schep and Bauer. We suggest a simple physical explanation of its source in the nanometer-thick oxide films relating it to strong local barrier-height fluctuations in the nearest to conducting electrodes layers of the insulator which are generated by oxygen vacancies in thin aluminum oxide tunnel barriers formed by thermal oxidation.

PACS numbers: 73.23.-b, 74.50.+r, 68.55.aj, 61.72.jd

Submitted to: *New J. Phys.*

1. Introduction

During the past decade, there has been considerable progress in understanding fundamental electronic properties of ultra-thin dielectrics, in particular, charge transport across disordered oxide layers. The increasing interest in such materials has been motivated by their promising applications as a gate dielectric in metal-oxide-semiconductor transistors instead of SiO_2 and a blocking dielectric for new-generation flash memory cells (see the papers [1, 2] and references therein) as well as a potential barrier for current carriers in superconducting tunnel junctions [3, 4]. In particular, it relates amorphous nanometer-thick alumina AlO_x. Unfortunately, in practice, high demands on the ultra-thin oxide films as current-blocking high-k dielectrics with a minimal dissipation are not usually fulfilled and a strong leakage current through the amorphous oxides is emerging as a potential limitation for most novel applications [1, 2, 4]. This finding has been often attributed to microscopic defects in the tunnel barrier with a greatly enhanced local transparency [5], commonly known as "pinholes". It has been assumed that the pinholes shunt the tunnel current and thus dominate the charge transport across the junctions. But a recent extensive analysis of a differential subgap conductance in highly resistive superconducting tunnel junctions with Al-oxide barriers [4] has ruled out the pinholes as the origin of the excess current, at least, in samples with normal conductance G_N per geometric area A between 10^4 and 10^7 $(\mathrm{Ohm{\cdot}cm^2})^{-1}$. Hence, the identification of charge transport mechanism in ultra-thin oxide films as well as the defects nature in amorphous dielectrics like AlO_x remains to be of great scientific and practical interest.

In this paper, we study charge transport across extremely thin AlO_x layers sandwiched between two metallic electrodes with specific normal conductance ranged in the interval from $2{\times}10^7$ to $7{\times}10^7$ $(\mathrm{Ohm{\cdot}cm^2})^{-1}$. It means that in our case the barrier thicknesses were significantly reduced comparing to those in the paper [4] and, hence, the presence of pinholes was more probable. Below, we not only reject the hypothesis about dominating role of microscopic pinholes in the ultra-thin oxide layers but use our experimental findings for four-layered Nb/Al-AlO_x-Nb junctions to show that the subgap resistance suppression in a superconducting state comparing to conventional tunnel junctions originates from a universal bimodal distribution of transparencies across the oxide barrier.

Concerning the latter statement, we should note that in the general case quantum transport through a mesoscopic physical system is determined by different factors like the system dimensionality, its size and shape, carrier density, and other sample-specific features. Universal transport properties, if they are, should be independent from microscopic details of particular materials and may include only a limited number of macroscopic characteristics. Inter alia, the universality can be expected for "dirty" systems with a very large spread of random potentials scattering current carriers. In the seminal paper by Schep and Bauer [6] the authors studied quantum transport properties of a single perfectly disordered interface (I) whose conductance is much smaller than

conductance of a ballistic conductor of the same cross-section and whose thickness d is sufficiently shorter than the Fermi wavelength $\lambda_{\rm F}$ in metallic bulks around it. They found that the distribution $\rho(D)$ of eigenvalues D of a transfer matrix connecting incoming and outgoing electronic modes (it is the product of the related transmission amplitude matrix and its Hermitian conjugate) does belong to a universality class and is given by an expression

$$\rho(D) = \frac{\hbar G_{\rm N}}{e^2} \frac{1}{D^{3/2}(1-D)^{1/2}}. \tag{1}$$

with $G_{\rm N}$, the disorder-averaged conductance. For a sample with such an interface any physical quantity f described by a linear statistics $f(D)$ (like conductance or shot noise power) can be calculated as $\int\limits_0^1 f(D)\rho(D)dD$.

The best way to study the distribution $\rho(D)$ in a nanometer-thick insulating film is to place it between two metallic layers and to measure current-voltage $I-V$ characteristics of the tunnel junction at very low temperatures when one or both electrodes are transformed into a superconducting (S) state. The reason consists in the fact that the shape of quasiparticle $I-V$ curves for SIS trilayers with a single quantum channel is extremely sensitive to the transmission probability [7] and, if the total current across the junction can be represented as a sum of independent contributions from individual transverse modes, its voltage dependence would be definitely determined by the function $\rho(D)$.

A first analysis of the $\rho(D)$ distribution in subnanometer-thick AlO_x layers using a superconducting heterostructure was performed by Naveh *et al.* [8] who measured current-vs-voltage and differential conductance-vs-voltage characteristics of planar highly conductive Nb-AlO_x-Nb trilayers at 1.8 K. In spite of the presence of an AlO_x barrier, the quasiparticle $I_{\rm qp}-V$ curves did not exhibit typical for conventional tunnel junctions behavior [7] with $R_{\rm sg} \gg R_{\rm N}$. Here $R_{\rm sg}$ is the junction differential resistance at voltages $|V| < 2\Delta/e$, known as a subgap resistance, Δ is the energy gap of a superconducting electrode, in this case, niobium, $R_{\rm N}$ is the trilayer normal-state resistance. On the contrary, the ratio $R_{\rm sg}/R_{\rm N}$ in the state when the Josephson critical current was totally suppressed by magnetic fields was near unity. Moreover, conductance-voltage curves exhibited well pronounced subharmonic gap structure known as a fingerprint of multiple Andreev reflections in high-transparent SIS samples [9, 10, 11]. All these findings were explained [8] as an impact of a broad double-peak distribution of Al-oxide barrier transparencies described by Eq. (1).

It should be noticed that the presence of a striking, polarity-independent deviation from standard single-particle tunneling $I-V$ curves in SIS junctions, is well known from 60s of the last century [12]. The subgap leakage was observed not only in highly conductive junctions [3] but also in low-transmission Nb-AlO_x-Nb trilayers [13] and in both cases evidences of an important role played by multiple Andreev-reflection processes have been reported [8, 4] although up to now it is not clear if their nature is identical or not [14]. Recently, there has been a resurgence of interest in this effect

since enhanced quasiparticle subgap conductance within individual junctions can cause decoherence effects in Josephson-effect-based superconducting quantum devices [15]. The "quality factor" of an SIS junction, which is usually defined by the ratio $R_{\rm sg}/R_{\rm N}$, is also important for low noise performance of SIS mixers and detectors where it is required to be at least ~ 15 for low noise performance [16]. At the same time, to achieve a broad rf-bandwidth, the junction must have a very high critical-current density $J_{\rm c}$ or a small $R_{\rm N}A$ product where A is the junction area [17]. The two requirements contradict each other because of a strong positive correlation between the "junction quality" and its specific conductance [3]. Another aspect of the same problem relates to the implementation of Josephson junctions operating in an overdamped mode when the ratio $R_{\rm sg}/R_{\rm N}$ should be suppressed as much as possible [18]. Since thermally oxidized aluminum oxide tunnel barriers provide the most reliable junction fabrication technology due to its reasonably good properties and comparatively easy fabrication [3], more fundamental knowledge about possibility to change the ratio $R_{\rm sg}/R_{\rm N}$ in a controllable way is needed in order to provide more insight into intrinsic structure of the AlO_x insulating layer [19] as well as into the nature of current fluctuations in related superconducting devices [20, 21].

Earlier investigations of subgap processes have been mainly concentrated on symmetric S-I-S [3] and asymmetric S-I-N [22] junctions. At the same time, it was stressed [23] that experimental studies of asymmetric S_1-I-S_2 devices can provide more information since the structure of I-V curves at voltages below $(\Delta_1 + \Delta_2)/e$ is more rich and pronounced [24, 25]. The aim of this work is to reexamine the conclusion of the paper [8] about very large variations of local barrier transparencies in nanometer-thick AlO_x layers, using asymmetric Josephson junctions with a proximity-coupled S/N bilayer as one of the device electrodes and studying the thermal effect in SNIS devices. Comparing with our previous experiments [26, 27, 18], we have enlarged the temperature interval studied, performing precise measurements of dissipative transport characteristics at temperatures significantly below and above 4.2 K. We have succeeded to extract corresponding $R_{\rm sg}/R_{\rm N}$ values and to compare them with our numerical simulations which are based on Eq. (1) applied to a more complicated than before four-layered junction geometry. Besides it, we present the data of novel rf-measurements proving the Josephson character of charge transport across our samples in a superconducting state. The rest of the paper is devoted to a simple physical interpretation of the Schep-Bauer distribution (1), the primary focus of the paper, relating it to strong local barrier-height fluctuations generated by oxygen vacancies in extremely thin Al-oxide films.

2. Experimental

We present experimental results obtained on asymmetric Nb/Al-AlO_x-Nb junctions developed at Instituto Nazionale di Ricerca Metrologica [26]. The main differences with a standard Nb-technology [28] are the following: the thickness of the Al interlayer

$d_{\rm Al}$ was increased from 5-10 nm up to 40-150 nm whereas the exposure dose, the product of the oxygen pressure and the oxidation time, was decreased from more than 1000 Pa·s down to 150-500 Pa·s (note that in the paper [4] oxygen doses varying from 1.7×10^3 to 8×10^5 Pa·s produced extremely thick barriers). Because of comparatively small exposure doses in our case, specific normal conductances of the Nb/Al-AlO$_x$-Nb devices were as high as (2 - 7)$\times10^7$ (Ohm·cm^2)$^{-1}$ which is of the same order of magnitude as those of highly-conductive symmetric SIS Josephson junctions studied by Naveh *et al.* [8]. Other details of our 25 μm^2-area junctions are given elsewhere [18].

Electrical measurements have been performed with a conventional four-terminal dc technique below critical temperatures of Nb/Al bilayers which were changed from 8 to 9 K for different $d_{\rm Al}$. All samples have exhibited supercurrents with values of 6 - 15 mA at 1.7 K, 3 - 8 mA at 4.3 K, and 1 - 5 mA at 6.0 K (left insets in figure 1). A typical current-voltage single-valued characteristic of a Nb/Al-AlO$_x$-Nb junction at finite temperatures is shown in the main panel of figure 2. It is well known [29] that the subgap current $I_{\rm sg}$ is a sum of three terms: a quasiparticle part $I_{\rm qp}$, a superconducting pair current $I_{\rm c}$, and an interference contribution. The latter two contributions can be made arbitrarily small if the critical current $I_{\rm c}$ is reduced by applying a magnetic field B. Then $I_{\rm sg} \approx I_{\rm qp}$. In our measurements of dissipative current-voltage characteristics, magnetic fields B up to 50 mT have been applied to the Nb/Al-AlO$_x$-Nb samples through a suitable coil. The $I_{\rm qp} - V$ curves have not been changed for two configurations of the magnetic fields (parallel and orthogonal to the current flow). The normal resistance $R_{\rm N}$ was determined from a linear fit to current-voltage curves with and without supercurrents at voltages above 1 mV (see figure 1) and the results of both estimations were in a good agreement with each other. It also agrees with the data for Nb-based trilayers [3] where specific conductance of thermally oxidized AlO$_x$ tunnel barriers was above 10^7 (Ohm·cm^2)$^{-1}$ for lowest oxygen exposure doses similar to ours. Subgap Ohmic resistance $R_{\rm sg}$ was extracted from experimental data as a slope of a best-fit linear regression line for quasiparticle curves in the interval from 0 to 0.2 mV where the subgap current increases near linearly with V (right insets in figure 1). The ratios $R_{\rm sg}/R_{\rm N}$ at 4.2 K were always of the order of unity as was found recently in our work on Nb/Al-AlO$_x$-Nb junctions with ultra-thin barriers [18] and before it for high-transparency symmetric Nb-AlO$_x$-Nb samples in [3]. Complementing our previous 4.2 K data for $R_{\rm sg}$ in SNIS junctions [18], in this work we have measured dissipative $I_{\rm qp} - V$ curves also at 1.7 and 6.0 K and increased the upper value of $d_{\rm Al}$ to 150 nm.

Below we analyze experimental data for five representative SNIS junctions with very different values of $d_{\rm Al}$, $R_{\rm N}$, $I_{\rm c}$, and products $I_{\rm c}R_{\rm N}$. It means that the samples had dissimilar Nb/Al interface resistances, as well as oxide barrier parameters, and our aim was to compare measured ratios $R_{\rm sg}/R_{\rm N}$ with those calculated using the universal distribution (1). Table 1 summarizes experimental characteristics of the samples whereas the main panel of figure 1 shows measured $I - V$ characteristics for one of the SNIS devices (dots) with two linear fits corresponding to $I = V/R_{\rm N}$ and $I = V/R_{\rm sg}$.

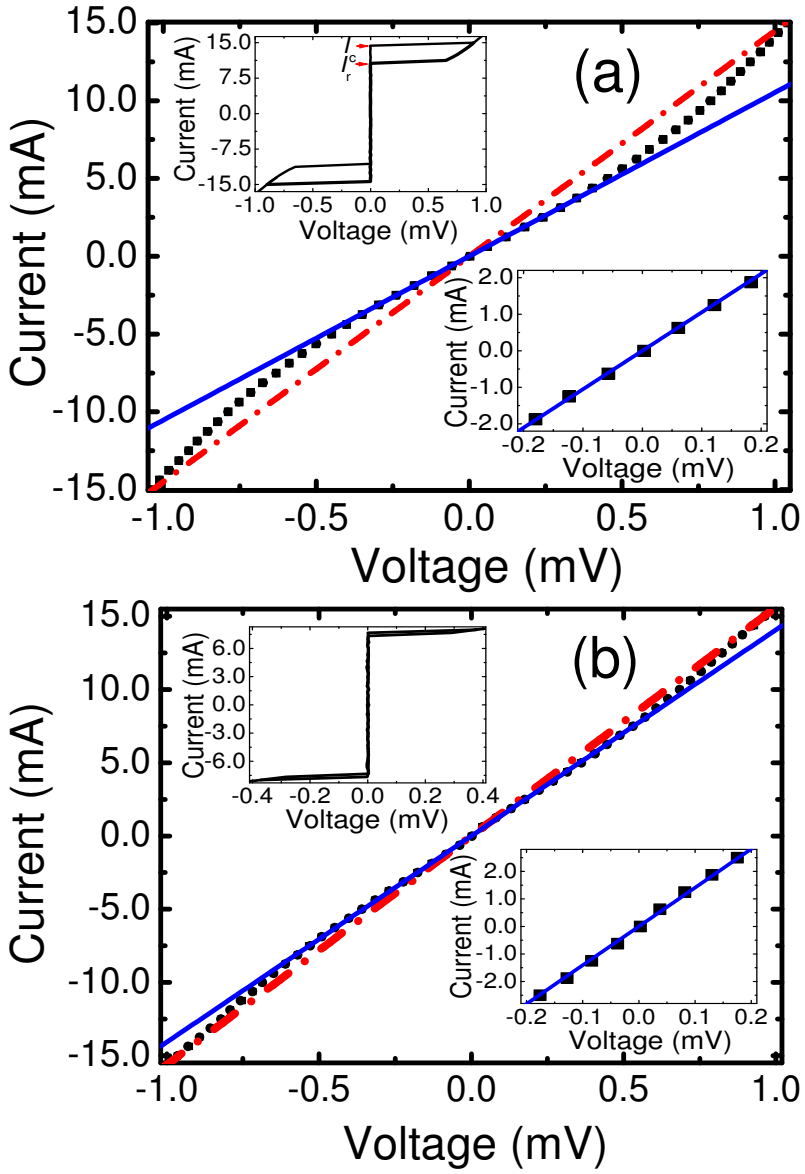

Figure 1. Dissipative current-voltage characteristics of a representative Nb/Al-AlO_x-Nb junction with $d_{Al} = 110$ nm at 1.7 K (a) and 4.3 K (b) measured in external magnetic fields about 50 mT applied to the tunnel sample through a suitable coil. Left insets demonstrate hysteretic behavior of the supeconducting current with switching I_c and retrapping I_r values whereas the main panels show quasiparticle $I_{qp} - V$ characteristics with suppressed Cooper-pair contribution (dotted curves). Right insets exhibit the same curves in an enlarged scale near $V = 0$. Solid and dashed-dotted straight lines correspond to Ohm's laws with $R_{sg} = 95$ mOhm and $R_N = 69$ mOhm at 1.7 K (a) and $R_{sg} = 71$ mOhm and $R_N = 64$ mOhm at 4.3 K (b).

3. Discussion

Conventional theory of tunneling effects in superconducting junctions [7] leads to the following conclusions relating the $I - V$ curves: first, at 1.7 K for $V \simeq 0.2$ mV the ratio

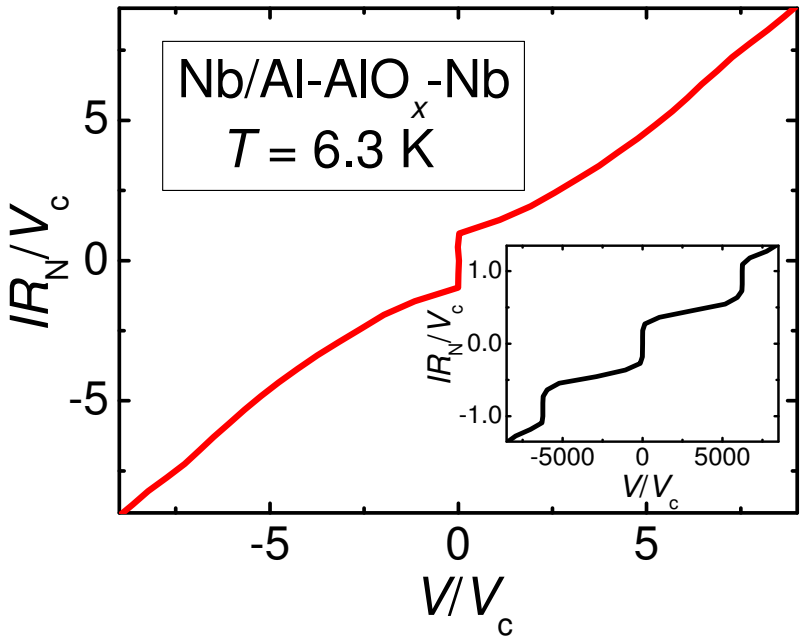

Figure 2. Typical current-voltage characteristic of a Nb/Al-AlO$_x$-Nb junction with 110 nm-thick Al interlayer (the main panel) and that of a binary-divided array of the same 8192 SNIS junctions under 73 GHz microwave irradiation (the inset). Critical currents I_c and the products $V_c = I_c R_N$ were about 2.2 mA and 0.2 mV, respectively at the operating temperature 6.3 K.

Table 1. Measured parameters for Nb/Al-AlO$_x$-Nb junctions with different Al thicknesses.

d_{Al} (nm)	$I_c(B=0)$, 1.7 K (mA)	R_N, 1.7 K (mOhm)	R_N, 4.3 K (mOhm)	R_N, 6.0 K (mOhm)	R_{sg}/R_N. 1.7 K	R_{sg}/R_N. 4.3 K	R_{sg}/R_N. 6.0 K
45	7.01	136	136	132	1.39	1.36	1.14
57	6.13	177	177	175	1.31	1.29	1.07
110	11.92	69	64	63	1.38	1.11	1.05
115	14.37	82	80	80	1.30	1.15	1.03
142	6.87	181	178	177	1.27	1.13	1.03

R_{sg}/R_N should be of the order of 10^5-10^6 in Nb-I-Nb samples and 10^2-10^3 in Nb/Al-I-Nb junctions, and second, the ratio has to decrease (exponentially for SIS contacts) with increasing temperature up to $\geq 10^2$ and $\leq 10^2$ at 4.3 K in Nb-I-Nb and Nb/Al-I-Nb devices, respectively. Our samples do not follow this behavior and exhibit (i) the ratio R_{sg}/R_N of the order of unity at all temperatures and (ii) a very weak temperature effect.

To conclude that these observations cannot be attributed to pinholes, we should prove a sinusoidal current-phase relation $I_s(\phi)$ for our junctions. One of the ways to check it is to detect Shapiro steps in the $I-V$ curves under microwave irradiation. Our experiments on SNIS single junctions rf radiated with frequency 73.5 GHz have

displayed a clear harmonic step structure in the current - voltage characteristics up to 8.3 K without any subharmonic features [30]. In the inset of figure 2 we show Shapiro steps at $T = 6.3$ K for binary divided series arrays of 8192 Josephson SNIS junctions with $d_{\rm Al} = 110$ nm, a part of the samples used for subgap resistance measurements.

It should be noticed that similar results for the ratio $R_{\rm sg}/R_{\rm N} \simeq 1$ and its universality have been already observed in symmetric Nb-AlO_x-Nb junctions and interpreted in the paper [8] following calculations [10, 11] where the validity of the Schep-Bauer distribution (1) was assumed and an effect of multiple Andreev reflections important for high transparencies D was taken into account. In particular, it follows from figure 2 in the paper [11] that in SIS trilayers the $R_{\rm sg}/R_{\rm N}$ value averaged over the voltage interval $|V| < \Delta_{\rm Nb}/e$ should be near 0.7 (the dashed line in figure 3). Experimental data for Nb-AlO_x-Nb samples (see figures 1 and 2 in the paper [8]) did well agree with this estimate. Our aim was three-fold: (i) to introduce an additional Al interlayer in order to modify the ratio $R_{\rm sg}/R_{\rm N}$ and to compare measured values with a calculated one; (ii) to change the thickness of the interlayer and to reveal in the experiment whether the distribution (1) comes from the disordered oxide layer or it is generated by diffusive charge transport in the N region, and (iii) to investigate for the first time the temperature dependence of the ratio $R_{\rm sg}/R_{\rm N}$.

In figure 3 we show experimental data for five representative samples which agree well with each other after normalization to $R_{\rm N}$. In contrast to the observations for Nb-AlO_x-Nb devices [8], the subgap resistance in our samples was higher than the normal-state value. To explain the findings, in figure 3 we show linear fits to results of such numerical calculations for two limiting cases of NIS and SIS junctions (dotted and dashed lines, respectively). The $I_{\rm qp} - V$ curve for an NIS trilayer was computed by us and that for an SIS structure was taken from the paper [11]. For comparison we plot the current-voltage characteristic in a normal state as well (dashed-dotted line).

We have also performed numerical simulations of the subgap resistance in SNIS junctions with arbitrary transparency D of the interspace between two superconducting electrodes and averaged the $I_{\rm qp} - V$ curves with the relation (1). Since our approach to the problem is based on numerical methods developed earlier [24, 25, 10, 11, 9, 31], we shall only briefly outline the main points of the calculations. The Nb/Al-AlO_x-Nb system studied is considered as an asymmetric S_1IS_2 junction where S_1 is the S/N bilayer. Proximized Nb layer induces in a thin Al film a superconducting order parameter which in the general case is a function of ε, the energy of a quasiparticle excitation in a superconductor measured from its Fermi level. The proximity effect changes the probability amplitude of a process of Andreev scattering $a_1(\varepsilon)$ from Al/Nb bilayer comparing with that from a bulk superconductor and this is just our main modification of the calculation scheme proposed in the papers referred above. The probability amplitude $a_1(\varepsilon)$ can be found if the ratio of modified and normal Green's functions F and G of a superconductor $\Phi(\omega) = \omega F(\omega)/G(\omega)$ (ω is the Matsubara frequency) is known. Note that in a bulk superconductor $\Phi(\omega)$ is equal to a constant order parameter Δ [32]. The function $\Phi(\omega)$ of a dirty normal metal placed in proximity

with a superconductor can be calculated using Usadel equations with corresponding boundary conditions [32]. In the following, we use a simplest approximation for the function $\Phi_{\rm Al}(\omega)$ in the Nb/Al bilayer $\Phi_{\rm Al}(\omega) = \Delta_{\rm Nb}/(1+\gamma\sqrt{\omega^2+\Delta_{\rm Nb}^2}/\Delta_{\rm Nb})$ with a fitting parameter γ and the energy gap of Nb $\Delta_{\rm Nb}$ [33]. The value of γ can be found by equating the gap magnitude in the Al interlayer calculated numerically to that found by us experimentally (for Al-film thicknesses studied its value at 1.7 K can be roughly estimated as 0.4 meV [27]). Then we are dealing with an S_1IS_2 junction where $a_1(\omega) = i\left(\omega - \sqrt{\omega^2+\Phi_{\rm Al}^2(\omega)}\right)/\Phi_{\rm Al}(\omega)$ and $a_2(\omega) = i\left(\omega - \sqrt{\omega^2+\Delta_{\rm Nb}^2}\right)/\Delta_{\rm Nb}$. At first, we consider a single-mode channel with a fixed transparency D between S_1 and S_2 electrodes. Its length is assumed to be much smaller than elastic and inelastic lengths. If so, we can describe the transport across the device in terms of Andreev-reflection amplitudes $a_{1,2}(\omega)$ and scattering characteristics of the barrier, namely, its transmission t ($|t|^2 = D$) and reflection r ($|r|^2 = 1-D$) probability amplitudes. The energy of an electron-like quasiparticle going across the barrier is increased by eV each time when it transfers the classically forbidden region, for example, from left to right, whereas that of an Andreev-reflected hole-like excitation increases moving in the opposite direction to the original electron. These scattering events will continue back and forth in the interspace between S_1 and S_2 superconductors and it is just a process of multiple Andreev reflections when each round trip of an electron-like quasiparticle increases its energy with a value of $2eV$. As a result, from each side of the barrier we get an infinite set of scattering states with different energies shifted by $2eV$ [10, 11]. By relating the wave functions at the two sides of the scattering region via scattering t and r amplitudes, we obtain recurrence relations for amplitudes of electron-like and hole-like wave functions in an asymmetric S_1IS_2 junction [24, 31] which have been solved numerically. After obtaining the scattering states, we calculate the electrical current $I_{\rm qp}(D,V)$ as a function of the applied voltage and the parameter D, taking into account that the contribution to the current from injected hole-like quasiparticles is equal to that from electrons. The total current-vs-voltage characteristic can be represented as a sum of independent contributions from individual transverse modes with a known distribution of their transmission probabilities $\rho(D)$: $I_{\rm qp}(V) = \int_0^1 dD\rho(D)I_{\rm qp}(D,V)$.

Reasonable agreement between the calculated $R_{\rm sg}/R_{\rm N}$ ratio and experimental data for Nb/Al-AlO$_x$-Nb junctions in figure 3 proves that, independently on the presence and on the thickness of the Al interlayer, the main spread of the transmission coefficients is related to the oxide barrier. Moreover, the Schep-Bauer distribution (1) not only qualitatively but also quantitatively describes the experimental data. As was expected, $R_{\rm sg}/R_{\rm N}$ values for the Nb/Al-AlO$_x$-Nb system are closer to those for NIS devices than to those for symmetric SIS junctions. From figure 3 it is clear that the approximation for $\Phi_{\rm Al}(\omega)$ used by us slightly exaggerates the proximity effect in Al.

Let us stress that while the $R_{\rm sg}/R_{\rm N}$ value is almost the same for different $d_{\rm Al}$ at 1.7 K, its temperature behavior, as follows from table 1, is strongly different. For the lowest $d_{\rm Al}$, the deviation of the ratio value at 4.3 K from that at 1.7 K is tiny whereas for larger

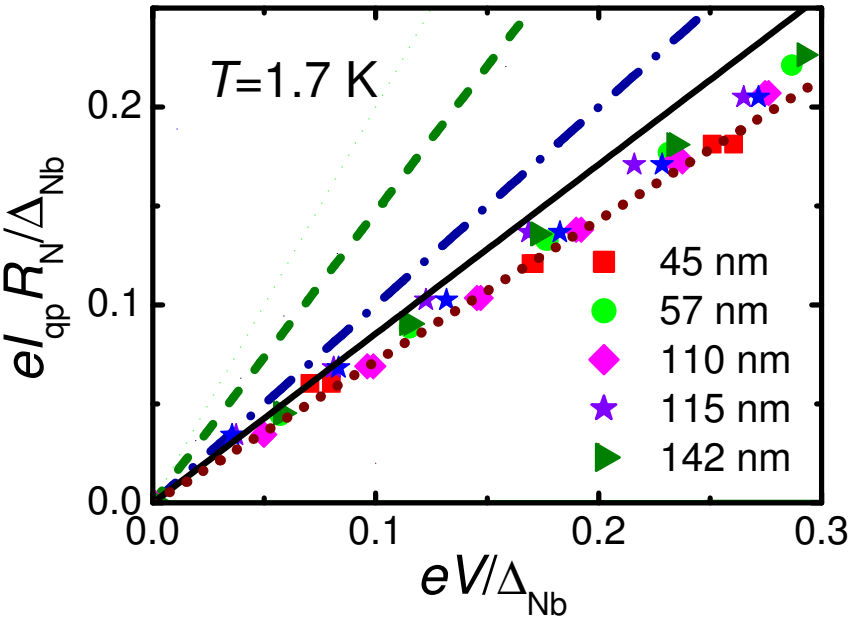

Figure 3. (Color online) Quasiparticle current-voltage characteristics of five Nb/Al-AlO_x-Nb junctions with different thicknesses of the Al interlayer (indicated in the figure) at 1.7 K (symbols) compared with linear fits to calculated dependences for NIS, SIS [11], SNIS, and NIN junctions with a disordered barrier layer (dotted, dashed, solid, and dashed-dotted lines, respectively).

thicknesses the R_{sg}/R_N value tends to unity. It can be explained as a result of a very different temperature behavior of the energy gap induced in an Al interlayer. It follows from figure 3 in the paper [27] that the temperature suppression of the induced gap and, hence, the asymmetry of SNIS superconducting junctions become stronger for thicker interlayers. As a result, in the subgap voltage range a strong peak evolves in $I-V$ curves for comparatively small barrier transparencies (see figure 5 in the paper [25]) and this thermally induced decrease of the subgap resistance is more effective for larger d_{Al}.

Disappearance of a hysteretic $I-V$ response in Nb/Al-AlO_x-Nb Josephson junctions when rising temperature from 1.7 K to 4.3 K (compare left insets in figures 1a and 1b) is partly an effect of the temperature influence on the R_{sg}/R_N ratio. It is well known [29] that the Josephson-device operation regime is governed by the McCumber-Stewart damping parameter

$$\beta_c = \frac{2e^2}{\hbar}\left(I_c R_N^2 C\right)\left(R_{sg}/R_N\right)^2 \qquad (2)$$

with C, the junction capacitance. If β_c is less than unity the current-voltage characteristic of the junction in a superconducting state is single valued like that shown in figure 1b. Otherwise, the response is hysteretic with switching I_c and retrapping I_r currents (figure 1a). We can estimate the β_c value for a representative junction shown in figure 1 using the Zappe's formula [34] $\beta_c = [2-(\pi-2)(I_r/I_c)]/(I_r/I_c)^2$. At 1.7 K we get $\beta_c = 2.21$. After increasing temperature to 4.3 K, the critical current decreased

from 11.0 to 6.9 mA, As a result, the McCumber-Stewart parameter due to Eq. (2) should reduce to 1.38. With an additional factor, temperature-induced decline of the R_{sg}/R_N ratio squared (Table 1), we obtain a final value $\beta_c = 1.07$ in agreement with the experiment showing a very small hysteresis in the current-voltage characteristics at 4.3 K (the left inset in figure 1b).

Let us now discuss the origin of universality of the distribution (1). We start with a simple parameterization $D(Z) = (1 + Z^2)^{-1}$ which follows directly from the delta-functional approximation for a potential barrier in a one-dimensional NIN trilayer [35] where $Z = k_F \int_0^d V_B(x)dx/E_F$, $V_B(x)$ and d are the local barrier height and the thickness of the insulating layer, k_F and E_F are the Fermi wave vector and the Fermi energy in a metallic electrode. To find the probability function for a transformed variable, we use a standard relation $\rho(Z) = \rho(D)(dD/dZ)$ and obtain that

$$\rho(Z) = 2\hbar G_N/e^2 = \text{const} \tag{3}$$

with Z uniformly ranging from zero to infinity. Thus, for very thin barriers Eq. (1) is equivalent to the assumption that an integral of the potential barrier height taken along an electron path inside the classically forbidden region is a uniform random variable (note that in a strongly disordered insulating layer such a path can significantly exceed the nominal barrier thickness d due to elastic subbarrier defect scatterings).

Even more, we cam conclude that the Schep-Bauer formula (1) for the transparency D is not limited to this assumption but is valid, independently on the physical nature, when (i) the transparency may be represented as a one-parameter Lorentzian and (ii) this parameter is uniformly distributed from very small up to very large values (see the related discussion concerning spatial distribution of barrier defects in the paper by Il'ichev *et al.* [36]). It is interesting that before the work [6] the same relation (1) was derived for a quasi-ballistic double-barrier INI interspace with two identical uniform insulating layers [37], a system which is physically very different from a thin disordered dielectric film. In our opinion, the reason for coincidence between the two systems consists in the fact that, for a finite thickness of the N interlayer d_N the transmission coefficient D is also of a Lorentzian-like form. To show it, we express the transmission amplitude $\tilde{t}$ across the I_1NI_2 transition region as a sum of a geometric series

$$\tilde{t} = t_1 \exp(i\varphi) t_2 (1 + r_1 \exp(2i\varphi) r_2 + ...) = \frac{t_1 \exp(i\varphi) t_2}{1 - r_1 \exp(2i\varphi) r_2}, \tag{4}$$

where $\varphi(\theta) = k d_N \cos(\theta)$ is the phase shift acquired by an electron with a wave number $\mathbf{k}$ traveling between two interlayer boundaries; $t_{1,2}(\theta)$ and $r_{1,2}(\theta)$ are transmission and reflection amplitudes for I_1 and I_2 insulating layers, respectively; θ is the injection angle between the vector $\mathbf{k}$ and the normal to layer interfaces. Then the probability of charge transition across the double-barrier I_1NI_2 trilayer can be expressed as $D(\theta) = (1 + \tilde{Z}^2(\theta))^{-1}$ with

$$\tilde{Z} = \sqrt{2 - |t_1|^2 - |t_2|^2 - 2\mathrm{Re}\left\{r_1 r_2 \exp(2i\varphi)\right\}} / \left(|t_1|\,|t_2|\right). \tag{5}$$

For a sufficiently large thickness d_N and symmetrical INI structure with low-transmission barriers $\tilde{Z}(\theta)$ is a rapidly oscillating function, which changes periodically from zero in

the resonance state to very high values. This very wide spread of the parameter $\tilde{Z}(\theta)$ is the reason why the two distributions coincide.

Now we transfer to experimental facts supporting the statement about a broad spread of local barrier transparencies in very thin dielectric layers and explaining its origin. First, we refer to a recent paper by Welander *et al* [38], where two ways of Al-oxide barrier formation in Nb/Al-AlO_x-Nb junctions were employed. The first process based on the conventional diffusion-limited oxidation of the Al layer yielded Josephson tunnel junctions with significant subgap leakage whereas the subgap currents in devices with layer-by-layer grown barriers agreed well with a standard tunneling theory. According to the paper [38] the extra conductance, most probably, comes from defects in the diffused Al oxide caused by room-temperature thermal oxidation of Al. These defects are known to be positively charged oxygen vacancies [19]. Another work [20] supporting the idea about the decisive role of oxygen vacancies is dealing with low-frequency noise measurements in Al-AlO_x-Al tunnel junctions. It was found that vacuum thermal annealing strongly reduces the $1/f$ noise level in the Al-based devices (sometimes, up to an order of magnitude). Since the $1/f$ noise phenomenon in metal-insulator-metal tunnel junctions is definitely related to slow filling and emptying of localized electron states in the barrier [39], the finding by Julin *et al.* [20] can be understood as a reduction of the charge traps number within the AlO_x layer by the annealing procedure.

Using conductive atomic force microscopy technique, Kim *et al.* [40] studied local tunneling properties of ultra-thin MgO films. Topographic maps showed that MgO layers were very flat whereas local tunnel current maps were strongly inhomogeneous with a number of current hotspots without any correlation between the two maps for the same sample. The most probable explanation can be that the tunnel current inhomogeneity arises from fluctuations in barrier height but not structural fluctuations. Comparing the maps before and after adding O_2 to the Ar plasma during MgO growth, the authors of the paper [40] argued that the inhomogeneity originates from oxygen vacancies. Elimination of certain oxygen defect populations leads to improved barrier heights with reduced spatial variations. Additional argument relating the presence of defect states in a very thin MgO tunnel barrier comes from the non-linearity of $I-V$ characteristics of corresponding magnetic tunnel junctions. The presence of oxygen vacancies in MgO leads to a new tunneling transport mechanism within the film when a charge is transported across the classically forbidden region via boson-induced tunneling jumps between randomly distributed localized states [41]. Combination of direct and inelastic tunneling events through the defects should lead to anomalous voltage dependence of the differential conductance in the form of a sum of power functions of V with different non-integer exponents. Such a behavior was just observed in the paper [42] for magnetic tunnel devices with MgO barriers. Very recent examples proving relation of anomalous properties of thin oxide layers to oxygen-originated inhomogeneities are given in the papers [1, 2]. Together with those discussed above they show that defects in disordered alumina are definitely related to oxygen although their detailed structure

remains unclear (of course, this statement is material-dependent).

But which physical quantity does mainly fluctuate in the disordered nanometer-thick oxide layers - the thickness d as was assumed in [22] or the average barrier height? By other words, in which way do the oxygen defects influence the tunnel current? The authors [43] paid attention to the role of metal-induced evanescent electronic states in the nearest to metal electrodes two-three layers of insulator unit cells. Inevitably random fluctuations in the electronic potential due to formation of oxygen defects should localize a substantial fraction of the evanescent states and, in our opinion, it is just the origin of strong local barrier strength variations within the insulating barrier. Let us emphasize that this scenario is exceptionally important just for ultra-thin oxide barriers as ours, since their thickness is expected to be of several unit cells and they directly contact metallic films from both sides.

In conclusion, highly-conductive asymmetric Nb/Al-AlO_x-Nb junctions show strong subgap leakage currents as was observed earlier in symmetric Nb-AlO_x-Nb trilayers [8] with high-transparency potential barriers similar to ours. Moreover, we have found that at 1.7 K the ratio of subgap to normal resistances does not greatly change for samples with Al-interlayer thicknesses ranging from 40 to 140 nm. This finding was explained as an indication of a universal distribution of barrier transparencies in ultra-thin Al oxide films. A noticeably reduced subgap leakage comparing with corresponding Nb-AlO_x-Nb trilayers [8] is in agreement with analogous finding for Nb/Al-AlO_x-Al samples with a 5 nm-thick interfacial Al film [15]. We do agree with the authors [15] that the magnitude of the leakage does not significantly depend on a particular material of the metallic layers. The temperature impact on the subgap junction resistance can be understood taking into account different temperature behavior of a superconducting energy gap induced in the proximized Al interlayer. Our results clearly indicate that in the case of ultra-thin and disordered Al-oxide films the main effect comes from the distribution of local oxide transparencies. Suppression of the subgap current with introducing the Al interlayer is caused by reducing the energy gap of one of the electrodes whereas the key factor, the universal distribution (1), remains almost the same as in Nb-AlO_x-Nb structures. We have argued that its presence originates from a very broad and homogeneous distribution of local barrier heights generated by oxygen vacancies within the Al-oxide film. If the defect distribution is more or less uniform [36], the integral of the potential barrier height along an electron path inside the barrier would be a uniform random variable. Of course, this phenomenon is not scale invariant. Since the depth of the penetration of metal-induced evanescent electronic states is limited to two-three atomic layers [43], leakage currents should be more pronounced for extremely thin insulating layers. The way to suppress it is to use dielectrics with lower band forbidden gap [16]. Because the effect is self-averaging, it will be more pronounced in devices with comparatively large junction area like ours. The latter remark explains why a noticeable reduction of the subgap current can be achieved by splitting a high-transparency micrometer-scale SIN heterostructure into several submicron sub-junctions [22].

Acknowledgements

This work was supported by a grant from Regione Piemonte. One of us (M.B.) would like to thank the National Institute of Metrological Research in Turin, Italy for support during the course of the work.

References

[1] Perevalov T V, Tereshenko O E, Gritsenko V A, Pustovarov V A, Yelisseyev A P, Park C, Han J H and Lee C 2010 *J. Appl. Phys.* **108** 013501
[2] Århammar C, Pietzsch A, Bock N, Holmström E, Araujo C M, Gråsjö J, Zhao S, Green S, Peery T, Hennies F, Ameriounb S, Föhlisch A, Schlappa J, Schmitt T, Strocov V N, Niklasson G A, Wallace D C, Rubensson J-E, Johansson B and Ahuja R 2011 *Proc. Natl. Acad. Sci. USA* **108** 6355
[3] Goodchild M S, Barber Z H and Blamire M G 1996 *J. Vac. Sci. Technol. A* **14** 2427
[4] Greibe T, Stenberg M P V, Wilson C M, Bauch T, Shumeiko V S and Delsing P 2011 *Phys. Rev. Lett.* **106** 097001
[5] Schrieffer J R and Wilkins J W 1963 *Phys. Rev. Lett.* **10** 17
[6] Schep K M and Bauer G E W 1997 *Phys. Rev. Lett.* **78** 3015
[7] Wolf E L 1989 Priciples of electron tunneling spectroscopy (New York: Oxford University Press)
[8] Naveh Y, Patel V, Averin D V, Likharev K K and Lukens J E 2000 *Phys. Rev. Lett.* **85** 5404
[9] Bratus' E N, Shumeiko V S and Wendin G 1995 *Phys. Rev. Lett.* **74** 2110
[10] Averin D and Bardas A 1995 *Phys. Rev. Lett.* **75** 1831
[11] Bardas A and Averin D V 1997 *Phys. Rev. B* **56** R8518
[12] Taylor B N and Burstein E 1963 *Phys. Rev. Lett.* **19** 14
[13] Milliken F P, Koch R H, Kirtley J R and Rosen J R 2004 *Appl. Phys. Lett.* **85** 5941
[14] Bezuglyi E V, Vasenko A S, Bratus E N, Shumeiko V S and Wendin G 2006 *Phys. Rev. B* **73** 220506(R)
[15] Im H, Pashkin Yu A, Kim Y, Li T F, Jung K, Astafiev O and Tsai J S 2010 *Physica C* **470** S832
[16] Endo A, Inoue H, Asayama S, Noguchi T, Kroug M and Tamura T 2008 *J. Phys.: Conf. Ser.* **97** 012251
[17] Kawamura J, Miller D, Chen J, Zmuidzinas J, Bumble B, LeDuc H G and Stern J A 2000 *Appl. Phys. Lett.* **76** 2119
[18] Lacquaniti V, De Leo N, Fretto M, Sosso A, Belogolovskii M 2010 *J. Appl. Phys.* **108** 093701
[19] Tan E, Mather P G, Perrella A C, Read J C and Buhrman R A 2005 *Phys. Rev. B* **71** 161401(R)
[20] Julin J K, Koppinen P J and Maasilta I J 2010 *Appl. Phys. Lett.* **97** 152501
[21] Faoro L and Ioffe L B 2007 *Phys. Rev. B* **75** 132505
[22] Lotkhov S V, Balashov D V, Khabipov M I, Buchholz F-I and Zorin A B 2006 *Physica C* **449** 81
[23] Ternes M, Schneider W-D, Cuevas J-C, Lutz C P, Hirjibehedin C F and Heinrich A J 2006 *Phys. Rev. B* **74** 132501
[24] Hurd M, Datta S and Bagwell P F 1996 *Phys. Rev. B* **54** 6557
[25] Hurd M, Datta S and Bagwell P F 1996 *Phys. Rev. B* **56** 11232
[26] Lacquaniti V, De Leo N, Fretto M, Maggi S and Sosso A 2007 *Appl. Phys. Lett.* **91** 252505
[27] Lacquaniti V, Belogolovskii M, Andreone D, Cassiago C, De Leo N, Fretto M and Sosso A 2010 *J. Phys.: Conf. Ser.* **234** 042018
[28] Gurvitch M, Washington M and Huggins H 1983 *Appl. Phys. Lett.* **42** 472
[29] Likharev K K 1991 Dynamics of Josephson junctions and circuits (Amsterdam: Gordon and Breach)
[30] Lacquaniti V, De Leo N, Fretto M, Sosso A, Müller F and Kohlmann J 2011 *Supercond. Sci. Technol.* **24** 045004

[31] Hurd M, Löfwander T, Johansson G and Wendin G 1999 *Phys. Rev. B* **59** 4412
[32] Golubov A A, Kupriyanov M Yu and Il'ichev E 2004 *Rev. Mod. Phys.* **76** 411
[33] Golubov A A, Houwman E P, Gijsbertsen J G, Krasnov V M, Flokstra J, Rogalla H and Kupriyanov M Y 1995 *Phys. Rev. B* **51** 1073
[34] Zappe H H 1973 *J. Appl. Phys.* **44** 1371
[35] Blonder G E, Tinkham M and Klapwijk T M 1982 *Phys. Rev. B* **25** 4515
[36] Ilichev E, Zakosarenko V, IJsselsteijn R P J, Hoenig H E, Meyer H-G, Fistul M V and Müller P 1999 *Phys. Rev. B* **59** 11502
[37] Melsen J A and Beenakker C W J 1994 *Physica B* **203** 219
[38] Welander P B, McArdie T J and Eckstein J N 2010 *Appl. Phys. Lett.* **97** 233510
[39] Rogers C T and Buhrman R A 1984 *Phys. Rev. Lett.* **53** 1272
[40] Kim D J, Choi W S, Schleicher F, Shin R H, Boukari S, Davesne V, Kieber C, Arabski J, Schmerber G, Beaurepaire E, Jo W and Bowen M 2010 *Appl. Phys. Lett.* **97** 263502
[41] Glazman L I and Matveev K A 1988 *Sov. Phys. JETP* **67** 1276; Xu Y, Ephron D and Beasley M R 1995 *Phys. Rev. B* **52** 2843
[42] Gokse A, Nowak E R, Yang S H and Parkin S S P 2006 *J. Appl. Phys.* **99** 08A906
[43] Choi S K, Lee D-H, Louie S G and Clarke J 2009 *Phys. Rev. Lett.* **103** 197001